

Invasive Micropapillary Carcinoma of the Breast: MR Imaging Findings

Hyo Soon Lim, MD¹, Cherie M. Kuzmiak, DO², Seo In Jeong, MD¹, You Ri Choi, MD¹, Jin Woong Kim, MD¹, Ji Shin Lee, MD³, Min Ho Park, MD⁴

Departments of ¹Radiology, ³Pathology and ⁴Surgery, Chonnam National University Medical School, Chonnam National University Hwasun Hospital, Hwasun 519-763, Korea; ²Department of Radiology, University of North Carolina at Chapel Hill, NC 27599-7510, USA

Objective: To analyze the magnetic resonance (MR) imaging findings of invasive micropapillary carcinoma of the breast.

Materials and Methods: MR images were retrospectively evaluated in 14 patients (age range: 37-67, mean age: 49 years) with pathologically confirmed invasive micropapillary carcinoma of the breast. The enhancement type (mass/non-mass), shape, margin, contrast enhancement, and time-intensity curve pattern on the dynamic study were correlated with the histopathologic features. Associated findings, such as edema, nipple change, skin change and enlarged axillary lymph nodes were also studied.

Results: The most common features of the masses were irregular shape (12 of 14 patients, 85.8%) and irregular or spiculated margin (11 of 14 patients, 78.7%). The contrast enhancement was heterogeneous in 11 patients (78.7%), rim enhancement in 2 cases (14.2%), and homogeneous in one patient (7.1%). The predominant kinetic pattern was rapid increase (14 of 14, 100%) in the initial phase and washout (11 of 14, 78.7%) in the delayed phase. Associated non-mass like enhancement was shown in 4 patients, representing ductal carcinoma *in situ*. MR imaging helped detect additional sites of cancer other than the index lesion in 3 patients (21.4%). Enlarged axillary lymphadenopathy was identified in 7 of the 14 patients (50%).

Conclusion: Invasive micropapillary carcinoma appears as a mass with an irregular shape, irregular or spiculated margin and heterogeneous enhancement on MR imaging. Though these findings are not specific and are also observed with other breast malignancies, invasive micropapillary carcinoma frequently showed multiple lesions, accompanying non-mass enhancement and axillary lymph node enlargement.

Index terms: Breast neoplasms; Diagnosis; Micropapillary carcinoma; Breast neoplasms; MR

INTRODUCTION

Invasive micropapillary carcinoma is a rare type of

invasive ductal carcinoma of the breast, accounting for 1.7-4% of breast cancers (1-4). Compared with ductal carcinoma, micropapillary carcinoma shows more distinctive architecture characterized by tufts of cells arranged in pseudopapillary structures devoid of fibrovascular cores and surrounded by empty, clear spaces lined by delicate strands of fibrocollagenous stroma (1). Although invasive micropapillary carcinoma is rare, it has clinical significance due to high frequency of lymphovascular invasion and axillary nodal metastasis, a greater degree of loco-regional recurrence and a poor prognosis (1, 3, 5). However, there is scant information about the radiologic features of invasive micropapillary carcinoma of the breast and most cases are

Received May 14, 2012; accepted after revision March 8, 2013.

Corresponding author: Cherie M. Kuzmiak, DO, Department of Radiology, University of North Carolina at Chapel Hill, 170 Manning Dr., Chapel Hill, NC 27599-7510, USA.

• Tel: (1919) 966-1081 • Fax: (1919) 966-1994

• E-mail: cherie_kuzmiak@med.unc.edu

This is an Open Access article distributed under the terms of the Creative Commons Attribution Non-Commercial License (<http://creativecommons.org/licenses/by-nc/3.0>) which permits unrestricted non-commercial use, distribution, and reproduction in any medium, provided the original work is properly cited.

described by their mammographic and sonographic features only. Magnetic resonance (MR) imaging examination of invasive micropapillary carcinoma of the breast is limited in the literature. Frequently, most cases of invasive micropapillary carcinoma exhibit a heterogeneous pattern of micropapillary forms mixed with the common forms of invasive ductal cancer (3). In this study, we included only the genuine type of invasive micropapillary carcinoma to better describe the radiologic features. The purpose of this study was to describe the MR imaging findings of genuine invasive micropapillary carcinoma of the breast and to correlate them with histopathologic features.

MATERIALS AND METHODS

The pathologic reports of patients with breast carcinoma at our institution between January 2007 and January 2011 were reviewed, and 21 cases of patients with pure invasive micropapillary carcinoma of the breast were found. Genuine invasive micropapillary carcinoma was defined as more than 90% of the tumor showing a micropapillary pattern. We excluded 6 patients who had not undergone preoperative MR imaging and one patient who had undergone pre-operative neoadjuvant chemotherapy. Consequently, 14 patients were included in this study. Eleven patients presented with a palpable breast mass and three patients were detected by a screening exam. MR imaging was performed to evaluate the tumor extent after diagnosis of breast cancer by sonographically guided 14-gauge automated core needle biopsy in all of the patients. All patients were women with the mean age of 49 years (range, 37-67 years). Of this, 10 patients underwent breast conservation surgery and 4 patients underwent mastectomy. The time interval between the breast MR imaging and surgical resection was 1-17 days (mean: 6 days). The institutional review board approved this retrospective study and did not require informed patient consent for review of their images and records.

Standard two-view mammography was performed using a Senographe 2000 D system (GE Healthcare, Milwaukee, WI, USA). Complementary views such as spot compression magnification views were obtained when necessary. Each mammographic lesion was reviewed according to the lesion type (mass only, mass with microcalcifications, microcalcifications only, focal asymmetry, architectural distortion), mass characteristics (shape and margin), distribution and morphology of microcalcifications using the criteria given by the American College of Radiology's

Breast Imaging Reporting and Data System (BI-RADS) (6). mammography was available for review for 12 patients whereas sonographic results were available for review in all patients. Each sonographic lesion was reviewed for characteristics of the mass (shape, margin, echo pattern, posterior acoustic features) and presence of calcifications, using the criteria given by the American College of Radiology's BI-RADS (7).

MR Imaging Technique

Breast MR imaging was performed in prone position using a dedicated surface breast coil with a 1.5-T (Signa Twin Speed Excite 1.5 T, GE Medical Systems, Milwaukee, WI, USA) and 3.0-T systems (Tim Trio, Siemens, Erlangen, Germany) in 5 and 9 patients respectively and included axillary lymph nodes from the level of the suprasternal notch line down. MR imaging consisted of a fat-suppressed, T1-weighted, T2-weighted fast spin echo, and gadolinium-enhanced images. MR imaging was performed with a 1.5-T MR scanner in 5 patients with the following parameters: axial fat-saturated T2-weighted spin echo images of bilateral whole breast (TR/TE, 4016.7/88.4; echo train length, 12; section thickness, 4 mm; field of view, 280 x 280 mm; matrix size, 288 x 256; gap, 1 mm; acquisition, 1) and sagittal fat-saturated T1-weighted images of bilateral whole breast (TR/TE, 700/9; echo train length, 0; section thickness, 4 mm; field of view, 180 x 180 mm; matrix size, 256 x 192; gap, 1 mm; acquisition, 1). After the initial examination, dynamic contrast-enhanced images were obtained by sagittal fat saturated T1-weighted spoiled gradient echo images with subtraction (3D-FLASH, TR/TE, 6.5/3.1; echo train length, 0; flip angle, 0; section thickness, 2.5 mm; field of view, 200 x 200 mm; matrix size, 256 x 256; no gap; acquisition, 1).

MR imaging was performed with a 3-T MR scanner in 9 patients with the following parameters: axial fat-saturated T2-weighted spin echo images of bilateral whole breast (TR/TE, 5200/79; echo train length, 21; section thickness, 4 mm; field of view, 320 x 320 mm; matrix size, 384 x 288; gap, 4.8 mm; acquisition, 1) and sagittal fat-saturated T1-weighted images of bilateral whole breast (TR/TE, 500/12; echo train length, 3; section thickness, 4 mm; field of view, 180 x 180 mm; matrix size, 320 x 224; gap, 1 mm; acquisition, 1). After the initial examination, dynamic contrast-enhanced images were obtained using axial fat saturated T1-weighted spoiled gradient echo images (TR/TE, 4.3/1.6; echo train length, 1; flip angle, 10; section thickness, 2 mm; field of view, 320 x 320 mm; matrix

size, 448 x 246; gap, 1 mm acquisition, 1). For dynamic contrast-enhanced images, a bolus injection of 0.1 mmol/kg of gadopentetate dimeglumine (Magnevist, Schering Berlin, Germany) was administered into the antecubital vein within 7-10 s, followed by a 16 mL saline flush. MR dynamic images, once before and five times after administration of contrast material, were obtained in bilateral whole breast at 40 s intervals.

After examination, standard subtraction images (un-enhanced images were subtracted from the early post-contrast images) and reverse subtraction images (last post-contrast images were subtracted from the early post-contrast images) were obtained on a pixel-by-pixel basis. The reformatted images with a maximum intensity projection were then created from the standard and reverse subtraction images. For enhancement kinetics analysis, time-intensity curves were plotted from the signal intensity values obtained in the regions of interest on serial dynamic images. To assess the early phase signal intensity increase, we evaluated the enhancement for the first post-contrast image at 60 s after injection of the contrast material.

Interpretation of the MR Imaging Findings

The breast lesions were analyzed using the BI-RADS MR lexicon (8). Areas of abnormal enhancement were described as mass or non-mass like enhancement. For the evaluation of the masses, MR images were reviewed for the evaluation of size, shape (round/oval, lobular, or irregular), margin (smooth, irregular, or spiculated), and contrast enhancement within the mass (homogeneous, heterogeneous, rim, central, enhancing internal septations, or dark internal septations), and the signal intensity. Shape and margin analysis was performed on the first post-contrast image. For non-mass like enhancements, MR images were reviewed for the evaluation of distribution (focal area, linear, ductal, segmental, regional, multiple regions, or diffuse) and internal enhancement (homogeneous, heterogeneous, clumped, stippled, or reticular/dendritic). The type of time-intensity curve was evaluated. The initial enhancement phase of the kinetic curve (slow, medium, or rapid) and the delayed phase of the kinetic curve (persistent, plateau, or washout) were also evaluated.

As defined by Liberman et al. (9), MR lesions were considered to be additional sites if they were located in a different breast quadrant than the index cancer, if they were in the same quadrant but were separated from the index cancer by at least 1.0 cm of intervening normal appearing

tissue on MR imaging, or if they were in the same quadrant and contiguous with the index cancer but extended at least 4.0 cm beyond the site of the index cancer.

Associated findings, such as edema, nipple change, skin change, and enlarged axillary lymph nodes, were also noted. Axillary lymph nodes that exhibited irregular contour, marked gadolinium enhancement and round hila and abnormal cortex were considered abnormal lymph nodes representing metastasis according to previously reported results. The sensitivity, specificity, positive predictive value, negative predictive value, and overall accuracy of MR imaging of axillary lymph node metastasis were calculated as sensitivity, $TP / (TP + FN)$; specificity, $TN / (TN + FP)$; positive predictive value, $TP / (TP + FP)$; negative predictive value, $TN / (TN + FN)$; and accuracy, $(TP + TN) / (TP + FP + FN + TN)$, where TP is the true-positive, TN the true-negative, FP the false positive and FN the false-negative.

Histopathology

A text search for invasive micropapillary was performed in the institutional pathologic database. All pathologic specimens were reviewed by a breast pathologist with 17 years of experience. In the present study, 10 patients underwent breast conserving surgery and 4 patients underwent modified radical mastectomy. The pathologist examined H and E-stained microscopic sections of the surgical specimen and interpreted the histopathologic findings are blinded of the MR imaging findings. Cases of tumor showing only small component of invasive micropapillary carcinoma were excluded and cases of tumor with more than 90% of the tumor showing a micropapillary pattern were included. The presence of associated ductal carcinoma *in situ* (DCIS), lympho-vascular invasion, and axillary lymph node status were evaluated. The MR imaging features were correlated with the histopathological findings by a single radiologist and a pathologist.

RESULTS

The age of 14 patients ranged between 37 and 67 years (mean age, 49 years). Physical examination revealed palpable, non-tender mass in 11 patients. Mammography was carried out in 12 patients in our institute and in two patients had the mammography at an outside institution and which were not available for review. Mammographic parenchyma as per the Breast Imaging Reporting and Data System lexicon was heterogeneously dense in six (50%)

patients, showing scattered fibroglandular densities in four (33.3%), and consisted of almost entirely fat in two (16.7%).

The mammographic findings of 12 patients consisted mass in 5 patients (41.7%) and mass with microcalcifications in 7 patients (58.3%) (Fig. 1). Multiple masses were detected in two patients. The mean diameter of these masses was

1.7 cm (range, 1.2-2.9 cm). The masses of 10 patients were irregular (83.3%) and two were oval (16.7%). The margins of the masses were spiculated in 6 (50%), ill-defined in 5 patients (41.7%) and microlobulated in one patient (8.3%). Microcalcifications were present in 7 patients and these microcalcifications were outside of the masses. The morphologic features of microcalcifications

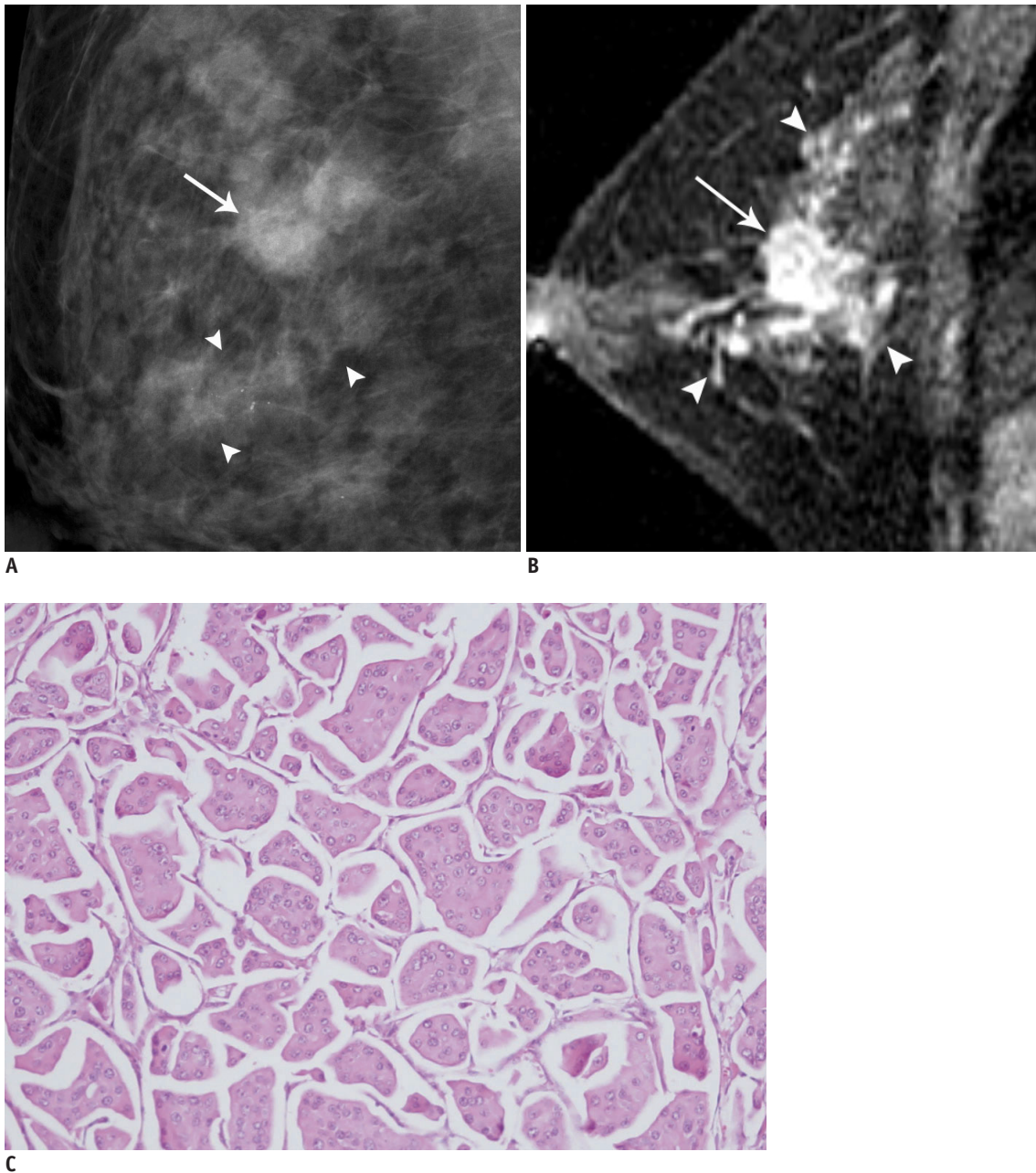


Fig. 1. Forty six-year-old woman with palpable mass in upper outer quadrant of right breast.

A. Mediolateral oblique mammogram shows irregular mass (arrow) and segmental distributed pleomorphic microcalcifications (arrowheads) outside of mass, extending anterior to mass. **B.** Early phase of dynamic enhancement MR imaging shows irregular, heterogeneously enhancing mass (arrow) with adjacent multiple regions of clumped enhancement (arrowheads) extending less than 4.0 cm, representing pathologically proven ductal carcinoma *in situ*. **C.** Photomicrograph of histopathological specimen (original magnification, x 100; hematoxylin-eosin stain) of tumor showed small cell clusters surrounded by empty spaces lined by delicate strands of stroma.

MR Imaging of Breast Invasive Micropapillary Carcinoma

were fine pleomorphic and amorphous in 5 patients (71.4%) and 2 (28.6%) patients respectively. The distribution was segmental in 4 (57.1%), regional in 2 (28.6%) and clustered in 1 (14.3%) patient. Suspicious axillary lymphadenopathy was identified with mammography in 1 of the 12 patients.

Sonography was performed in all the patients including sonographically guided percutaneous 14-gauge core needle biopsy. In sonographic analysis, all cases showed irregular hypoechoic masses with a not-circumscribed margin. Multiple irregular hypoechoic masses were seen in 4 patients. In 2 patients, additional irregular hypoechoic masses were also detected on sonography that were clinically and mammographically occult. In 5 patients, calcifications were seen as bright punctuate echoes within an irregular and indistinct hypoechoic mass. MR imaging was performed to evaluate the tumor extent after the diagnosis of the breast cancer.

MR imaging was useful in detecting all 14 invasive micropapillary carcinomas which are summarized in Table 1. The most common features of the masses were irregular shape (12 of 14, 85.8%) and irregular or spiculated margin (11 of 14, 78.7%) (Fig. 1). Contrast enhancement within the mass was heterogeneous in 11 (78.7%) and rim enhancement in 2 (14.2%) patients. The predominant kinetic pattern was rapid increase (14 of 14, 100%) in the initial phase and washout (11 of 14, 78.7%) in the

delayed phase. Associated non-mass like enhancement was shown in 4 patients (Fig. 1). In 3 patients, segmental or regional distributed microcalcifications on mammography were seen as non-mass like enhancement on MR imaging. The enhancement pattern of non-mass like enhancement was segmental clumped enhancement, multiple regional clumped, regional stippled and focal clumped enhancement were seen one patient each, representing the presence of accompanying DCIS. Additional sites of cancers other than the index lesion were detected in 3 patients (21.4%) (Fig. 2). Two lesions were in the same quadrant and one was in a different quadrant. Targeted sonography revealed a sonographic correlate in two patients and sonographically guided localization was performed. Mastectomy was needed for one patient. Suspicious axillary lymphadenopathy was identified with MR imaging in 7 of the 14 patients (50%).

Breast conserving surgery was performed in 10 patients and 4 patients underwent modified radical mastectomy. Axillary lymph node dissection was performed in 11 of 14 patients and sentinel lymph node biopsy was performed in 3 patients. Breast cancer stage was stage I in 2 (14.3%), stage II in 7 (50%) and stage III in 5. Based on histopathologic examination, we included the cases with more than 90% of the tumor consisting of invasive micropapillary pattern. Associated DCIS was found in 11 of the 14 patients (78.6%), usually mixed histologic type with cribriform, solid, and micropapillary patterns. One patient had bilateral breast cancer, and invasive ductal carcinoma, not otherwise specified, was diagnosed in the contra-lateral breast. Lympho-vascular invasion was found in 9 of the 14 patients (64.3%). Axillary lymph node metastases were found in 10 of the 14 patients (71.4%). The sensitivity, specificity, positive predictive value, negative predictive value, and overall accuracy of MR imaging of axillary lymph node metastasis were 60, 75, 85.7, 42.9, and 64.3%, respectively.

Follow-up data were available for 14 patients (12-42 months). Hepatic metastases was detected in one patient at 34 months after the initial diagnosis. Locoregional recurrence in mastectomy site with hepatic and lung metastases was detected in one patient at 20 months after the initial diagnosis.

DISCUSSION

Invasive micropapillary carcinoma of the breast is a distinct histologic type of invasive carcinoma, that was first

Table 1. MR Imaging Findings of Invasive Micropapillary Carcinoma of Breast

Features		Number of Tumors (%)
Shape	Round	0
	Oval	1 (7.1)
	Lobular	1 (7.1)
	Irregular	12 (85.8)
Margin	Smooth	3 (21.3)
	Irregular	5 (36.1)
	Spiculated	6 (42.6)
Enhancement	Homogeneous	1 (7.1)
	Heterogeneous	11 (78.7)
	Rim enhancement	2 (14.2)
	Central enhancement	0
Associated non-mass like enhancement	Segmental clumped	1 (7.1)
	Multiple regional clumped	1 (7.1)
	Regional stippled	1 (7.1)
	Focal clumped	1 (7.1)
Kinetic curve (delayed phase)	Persistent	2 (14.2)
	Plateau	1 (7.1)
	Washout	11 (78.7)

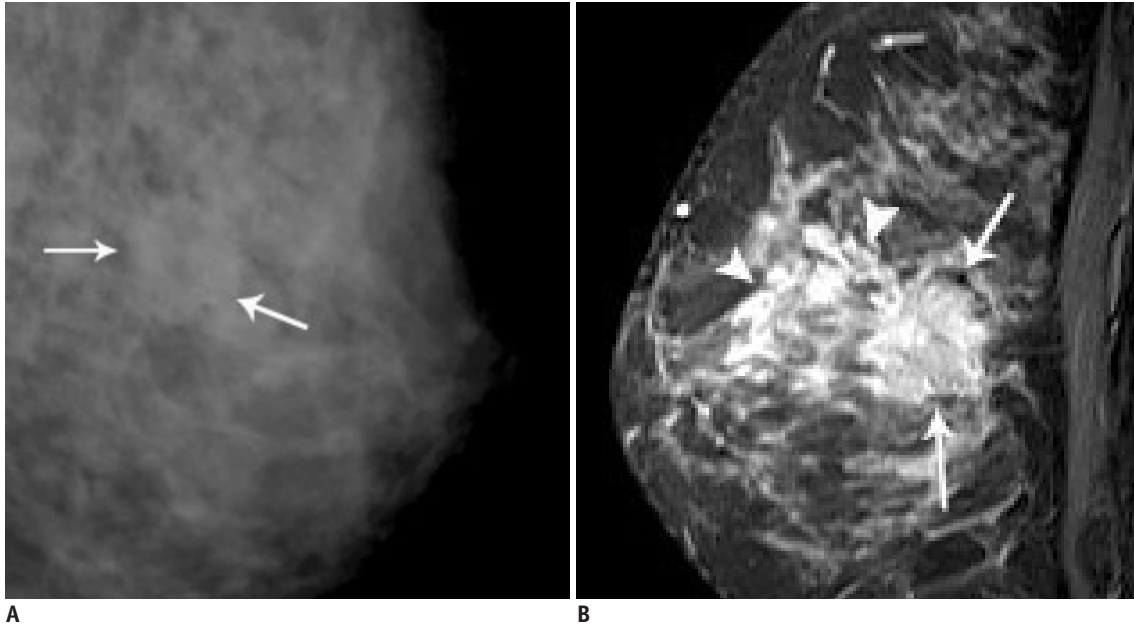


Fig. 2. Thirty nine-year-old woman with palpable mass in left breast.

A. Mediolateral oblique mammogram shows irregular equal density mass in left breast corresponding to area of palpation (arrows). **B.** Dynamic enhancement MR imaging shows irregular heterogeneously enhancing mass (arrows) with segmental clumped enhancement (arrowheads) extending 4 cm anterior to known invasive cancer. MR imaging found additional site. Mastectomy revealed invasive micropapillary carcinoma with extensive ductal carcinoma *in situ*.

described by Siriaunkgul and Tavassoli (10), characterized by a distinctive growth pattern of small, tightly cohesive cell clusters disposed within spaces resembling lymphatic vessels. Immunohistochemically, invasive micropapillary carcinoma exhibits the 'inside-out' pattern of epithelial membrane antigen expression (1). However, often most invasive micropapillary carcinomas show a heterogeneous pattern of invasive micropapillary pattern with a common type of invasive cancer (3). If the invasive micropapillary pattern was found throughout the lesion, the term genuine invasive micropapillary carcinoma is used and if the pattern was found as part of an otherwise conventional invasive ductal carcinoma, mixed invasive micropapillary carcinoma is used. If more than 90% of the tumor consisted of a micropapillary pattern, that tumor was classified as genuine invasive micropapillary carcinoma and included in this study.

To our knowledge, there is a limited amount of published information on the radiologic findings of pure invasive micropapillary carcinoma of the breast (11, 12). Günhan-Bilgen et al. (11) reported the mammographic and sonographic findings of 16 pure invasive micropapillary carcinomas with spiculated, irregular or round, high density mass with or without associated microcalcifications. Sonography examinations revealed homogeneously hypoechoic, irregular or microlobulated mass with posterior

acoustic shadowing or normal sound transmission. A study by Adrada et al. (12) suggested that the lesion was a high-density irregular mass associated with microcalcifications on mammogram and a solid irregular hypoechoic mass with indistinct margins and frequent axillary nodal involvement on sonogram. Microcalcifications were representative of an associated DCIS component. The imaging characteristics were highly suggestive of malignancy in both studies.

However, few studies on the MR imaging findings of invasive micropapillary carcinoma of the breast exist; however, the number of patients in these studies was also small. Adrada et al. (12) reported the MR imaging findings of invasive micropapillary carcinoma of the breast in 5 lesions; four enhancing masses were present in three patients and non-mass like enhancement was found in two patients. The masses showed an irregular shape and spiculated margins. Similarly, Kubota et al. (13) reported the MR imaging findings of 8 breast carcinomas with a variable proportion of invasive micropapillary carcinoma. They compared the radiological imaging features of 8 invasive micropapillary carcinomas and 22 other types of invasive ductal carcinomas. There was no predictive descriptor in the BI-RADS lexicon for invasive micropapillary carcinoma on mammography and sonography. They found that invasive micropapillary carcinoma showed a characteristic irregular shaped mass on MR imaging more frequently

than other types of invasive ductal carcinomas. In a case report, MR imaging findings indicated breast cancer with an extensive intraductal component (14). In the present study, we included only genuine invasive micropapillary carcinoma patients with most predominant features of the masses were irregular shape (12 of 14, 85.8%), irregular or spiculated margin (11 of 14, 78.7%) and heterogeneous contrast enhancement (78.7%). The MR imaging findings of invasive micropapillary carcinoma were highly suggestive of malignancy. In addition to the mass, associated non-mass like enhancement was detected in 4 patients and this was pathologically proven to be accompanying DCIS.

Although MR imaging findings of invasive micropapillary carcinoma are not specific and may be seen with other breast malignancies, MR imaging detected additional sites in 3 of 14 patients (21.4%) and defined the tumor extent more accurately than mammography. In one patient, an additional mass that was detected in a different breast quadrant than the index cancer was not seen on mammography, and this was pathologically proven to be DCIS. In one patient, an additional enhancing mass was detected in the same quadrant however, it was separated from the index cancer by 1.5 cm of intervening normal appearing tissue on MR imaging. In one patient, segmental clumped enhancement was present and contiguous with the index cancer but extended 4.0 cm beyond the site of the index cancer, suggesting the presence of DCIS. Subsequently, due to the MR imaging findings, a change in management was made. Invasive micropapillary carcinoma frequently showed multiplicity. Walsh and Bleiweiss (15) reported invasive micropapillary carcinoma was multifocal in 25 of 80 cases (31.4%).

Accompanying DCIS was found in 11 of the 14 patients (78.6%) as it was usually of mixed histologic type with cribriform, solid, and micropapillary patterns. The most frequent intraductal component was of the micropapillary type in the study by Walsh and Bleiweiss (15) but typically had intermediate to high-grade nuclei and necrosis. Adrada et al. (12) reported that 26 of 28 patients (93%) had an intraductal component, usually of mixed type with cribriform, solid, and micropapillary patterns.

Invasive micropapillary carcinoma has a high frequency of axillary lymph node metastasis, with reports of 66.6-90.5% (3, 16, 17). Walsh and Bleiweiss (15) reported that small micropapillary carcinomas seem to show the same proclivity for lymphatic spread and nodal dissemination as larger micropapillary carcinomas despite their minute size,

and invasive micropapillary carcinomas less than 5 mm in size exhibited lymph node metastasis at a rate of 75%. As suggested by previous studies, it is not the tumor size or the amount of the invasive micropapillary carcinoma component in the tumor, but the histologic features and stromal reactions that correlate with the aggressiveness of the tumor (18). It has been proposed that the histologic grade, lymphatic vessel density, and lymphocyte infiltration of invasive micropapillary carcinoma may be the key factors that influence lymph node metastasis (18). In this study, lympho-vascular invasion was found in 9 of 14 patients (64.3%) and axillary lymph node metastases were found in 10 of 14 patients (71.4%). The diagnosis of axillary lymph node metastasis, the sensitivity, specificity, positive predictive value, negative predictive value, and overall accuracy of MR imaging were 60, 75, 85.7, 42.9, and 64.3%, respectively. This result suggests that patients with invasive micropapillary carcinoma have a high possibility of axillary lymph node metastases regardless of the radiologic findings and require pathologic examination of the axillary lymph nodes.

In conclusion, invasive micropapillary carcinoma was presented as a mass with an irregular shape, irregular or spiculated margin and heterogeneous enhancement and frequently showed multiple lesions, accompanying non-mass enhancement and axillary lymph node enlargement. The present study suggest that, MR imaging may be an important diagnostic tool for defining the extent of the tumor and excluding the possibility of multiplicity, which would not be apparent through mammography or sonography.

REFERENCES

1. Luna-Moré S, Gonzalez B, Acedo C, Rodrigo I, Luna C. Invasive micropapillary carcinoma of the breast. A new special type of invasive mammary carcinoma. *Pathol Res Pract* 1994;190:668-674
2. Paterakos M, Watkin WG, Edgerton SM, Moore DH 2nd, Thor AD. Invasive micropapillary carcinoma of the breast: a prognostic study. *Hum Pathol* 1999;30:1459-1463
3. Kuroda H, Sakamoto G, Ohnisi K, Itoyama S. Clinical and pathologic features of invasive micropapillary carcinoma. *Breast Cancer* 2004;11:169-174
4. Pettinato G, Manivel CJ, Panico L, Sparano L, Petrella G. Invasive micropapillary carcinoma of the breast: clinicopathologic study of 62 cases of a poorly recognized variant with highly aggressive behavior. *Am J Clin Pathol* 2004;121:857-866

5. Yu JI, Choi DH, Park W, Huh SJ, Cho EY, Lim YH, et al. Differences in prognostic factors and patterns of failure between invasive micropapillary carcinoma and invasive ductal carcinoma of the breast: matched case-control study. *Breast* 2010;19:231-237
6. American College of Radiology. *Mammography*. In: Breast imaging reporting and data system (BI-RADS), 4th ed. Reston, VA: American College of Radiology, 2003
7. American College of Radiology. *Ultrasound*. In: Breast imaging reporting and data system (BI-RADS), 4th ed. Reston, VA: American College of Radiology, 2003
8. American College of Radiology. *MRI*. In: Breast imaging reporting and data system (BI-RADS), 4th ed. Reston, VA: American College of Radiology, 2003
9. Liberman L, Morris EA, Dershaw DD, Abramson AF, Tan LK. MR imaging of the ipsilateral breast in women with percutaneously proven breast cancer. *AJR Am J Roentgenol* 2003;180:901-910
10. Siriaunkgul S, Tavassoli FA. Invasive micropapillary carcinoma of the breast. *Mod Pathol* 1993;6:660-662
11. Günhan-Bilgen I, Zekioglu O, Ustün EE, Memis A, Erhan Y. Invasive micropapillary carcinoma of the breast: clinical, mammographic, and sonographic findings with histopathologic correlation. *AJR Am J Roentgenol* 2002;179:927-931
12. Adrada B, Arribas E, Gilcrease M, Yang WT. Invasive micropapillary carcinoma of the breast: mammographic, sonographic, and MRI features. *AJR Am J Roentgenol* 2009;193:W58-W63
13. Kubota K, Ogawa Y, Nishioka A, Murata Y, Itoh S, Hamada N, et al. Radiological imaging features of invasive micropapillary carcinoma of the breast and axillary lymph nodes. *Oncol Rep* 2008;20:1143-1147
14. Ota D, Toyama T, Ichihara S, Mizutani M, Kamei K, Iwata H. A case of invasive micropapillary carcinoma of the breast. *Breast Cancer* 2007;14:323-326
15. Walsh MM, Bleiweiss IJ. Invasive micropapillary carcinoma of the breast: eighty cases of an underrecognized entity. *Hum Pathol* 2001;32:583-589
16. Luna-Moré S, Casquero S, Pérez-Mellado A, Rius F, Weill B, Gornemann I. Importance of estrogen receptors for the behavior of invasive micropapillary carcinoma of the breast. Review of 68 cases with follow-up of 54. *Pathol Res Pract* 2000;196:35-39
17. Nassar H, Wallis T, Andea A, Dey J, Adsay V, Visscher D. Clinicopathologic analysis of invasive micropapillary differentiation in breast carcinoma. *Mod Pathol* 2001;14:836-841
18. Guo X, Chen L, Lang R, Fan Y, Zhang X, Fu L. Invasive micropapillary carcinoma of the breast: association of pathologic features with lymph node metastasis. *Am J Clin Pathol* 2006;126:740-746